Curing Behavior, Mechanical Properties, Intermolecular Interaction, and Morphology of Silicone/Polypyrrole/Polymer Electrolyte Composites

Hsien-Tang Chiu, Jyh-Horng Wu

Graduate school of Polymer Engineering, National Taiwan University of Science and Technology, Taipei, Taiwan 106, Republic of China

Received 26 February 2005; accepted 20 April 2005
DOI 10.1002/app.21334
Published online in Wiley InterScience (www.interscience.wiley.com).

ABSTRACT: The curing behavior, mechanical properties, intermolecular interaction, and morphology of silicone, polypyrrole, and polymer electrolyte composites were studied. A rigid-body pendulum rheometer was used to determine the curing behavior of silicone/PEL blends. The polymer structure was evaluated using FTIR and Differential Scanning Calorimetery. The mechanical properties, including stress, strain, and hardness, were measured using a material testing system. The morphology of the composites was measured using scanning electron micrographs. The intermolecular interaction of the composites was measurement using dynamic mechanical analysis. The results show that the curing reaction rate is fast upon addition of 10 wt % of polymer electrolyte for silicone. The linear molecular structure of the polymer electrolyte was wound around the silicone polymer network structure forming a semi-interpenetrating network. The intermolecular interaction was influenced by the composites, and the Ppy film effect on the surface of SP10 blends is more uniform than that of silicone. © 2006 Wiley Periodicals, Inc. J Appl Polym Sci 101: 2754–2764, 2006

Key words: silicone; polypyrrole; polymer electrolyte; composites; curing behavior; intermolecular interaction

INTRODUCTION

Electrical conductivity is important in many rubber and plastic composites for antistatic applications, wire and cable sheating, shielding against electromagnetic interference, capacitive vedio disks, electrically conductive pipes, radiofrequency shielding, surface electrode for biomedical applications, and temperature-sensitive resistors, which are some typical applications. Silicone rubber can be used for extensive applications, and the characteristics of silicon oxide revealed are like low T_g,[1,2] high-impact resistance,[3,4] thermal stability,[5,6] high mechanical and chemical resistance, weatherproofing, ozone resistance, and radiation resistance.[7,8] It is widely applied in various industrial products. The application of polymer electrolytes is very broad. It is used in such products including solid-state batteries, sensors, and display devices.[9–14] Polypyrrole (Ppy) has superiority for commercial application, stability in air, and ease of preparation.

In many of the past studies, silicone has been an insulator to which conductivity is imparted by the addition of finely divided fillers (such as carbon black)[15–20] and conductive polymer (such as Ppy)[21,22] of high intrinsic conductivity. Princy et al.[17] reported the effect of different types of carbon blacks, copper powder, and graphite on electrical conductivity and mechanical properties of silicone rubber compounds. Kost et al.[18–20] have reported on resistivity changes during mechanical loading of carbonate black-filled silicone rubber specimens. The modes of loading under study were axial tension, relaxation, cyclic load in tension, and an analytical model to describe resistivity–strain–time relations was proposed. Gan et al.[21] reported the synthesis of a new conducting interpenetrating polymer network based on silicone crosslinked styrene–isoprene–styrene triblock copolymer and polypyrrole. Kim et al.[22] report the direct covalent junction between a conductive polypyrrole film and silicon using a reaction that attaches pyrrole units directly to the silicon surface.

In this study, we use the Ppy by *in situ* polymerization (chemical oxidation) on the blend surfaces of silicone and the semi-interpenetrating network (semi-IPN) based on silicone and polymer electrolytes (polypropylene oxide–polyethylene oxide copolymer with $LiClO_4$ 20 wt %, PEL). The curing behavior, mechanical properties, intermolecular interaction, and morphology of silicone/PEL/Ppy composites were examination.

Correspondence to: H.-T. Chiu (D9004201@mail.ntust.edu.tw).

© 2006 Wiley Periodicals, Inc.

TABLE I
The Compositions of Silicone/PEL Blends with PEL Contents

	Wt %				
Material/Code No.	Silicone	SP5	SP10	SP15	SP20
Silicone	100	95	90	85	80
PEL	—	5	10	15	20

EXPERIMENTAL

Materials

The materials were silicone (Polydimethylsiloxane, model No. 9050) manufactured by Dow Corning) and poly electrolyte liquid, which is a polypropylene oxide–polyethylene oxide copolymer with $LiClO_4$ 20 wt % (PEL) manufactured by Japan Carlit. The hardening agent product name was CORONATE HX, manufactured by the Nippon Polyurethane Industry Co. Ltd. Pyrrole was manufactured by JANSSEN in a 99%, Acetonitrile [(CH_3CN), OSAKA 99%] aqueous solution. The oxidizing agent ammonium was peroxodisulfat [$(NH_4)_2S_2O_8$], which was manufactured by FERAK.

Sample preparation

The sample for testing was produced through the even mixing of silicone and PEL in accordance with the mixing proportions specified in Table I and through its placement in a mold. After being soaking in a vacuum for a 30 min, the mold was kepy at 150°C for 30 min. Upon cooling, the test sample was removed from the mold and trimmed to the proper size for testing. In addition, choice silicone and SP10 were blended in a B stage. The mixture was soaked in 6*M* solution with acetonitrile for 10 min. The test sample was then removed and placing into 0.1*M* ammonium peroxodisulfat [$(NH_4)_2S_2O_8$] solution for 10 min. The dip-coating process was repeated four times. The test piece, coated with black and even Ppy film on the surface, was obtained after curing at 150°C for 10 min.

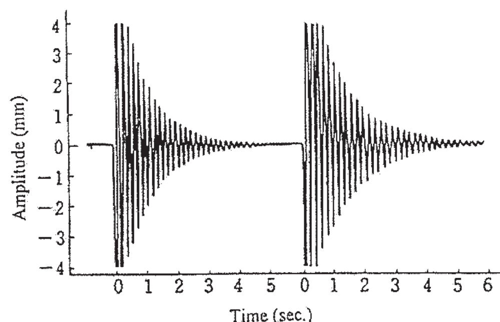

Figure 2 Change in vibration wave in curing process.

Measurements

Principle of the rigid-body pendulum rheometer (RPR)[23,24]

For a practical test of the curing process, the testing method made use of a damping pendulum system in compliance with the specifications of ISO 1522. To measure the curing process, a rigid-body pendulum equipped with a knife edge was provided. The test piece, coated or set on a plate, was placed on a heating mount, and the pendulum was set so that the edge, or the fulcrum of the swing, came vertically in contact with the coated surface (Fig. 1).

When an external force was applied by a magnetic adsorption force to the pendulum, the pendulum started to vibrate freely. Both sides of the edge of the pendulum yielded the strain of compression and elongation of the coated test piece. As a result, the viscoelastic property of the test pieces caused the swinging period of the pendulum and the swing damping action. Through the measurement of the logarithmic

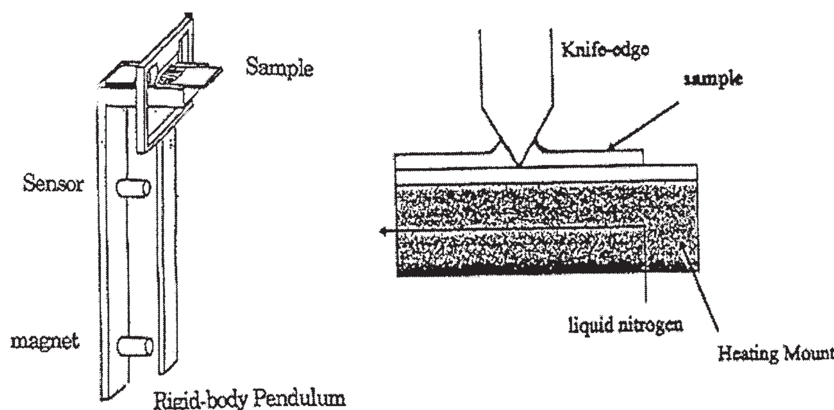

Figure 1 System of the instrument.

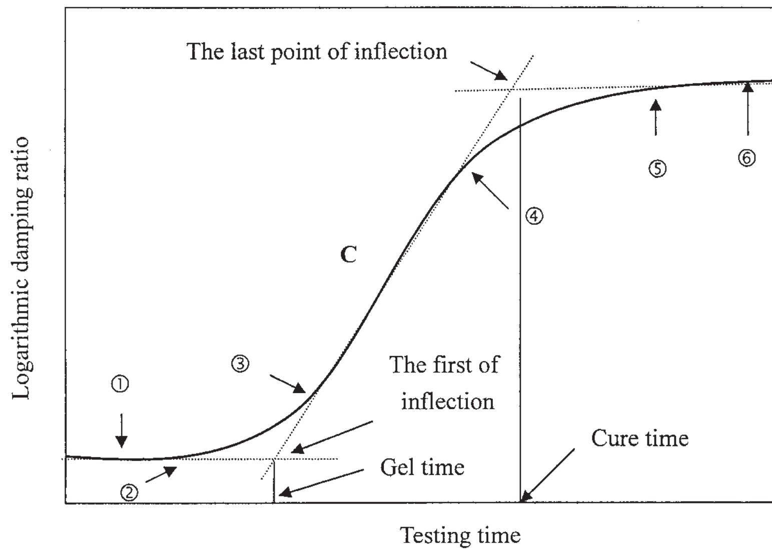

Figure 3 The curing behavior of a type of rigid-body pendulum rehometer.

damping ratio (Δ), the curing behavior of the test piece could be obtained with the following equation:

$$\Delta = [\ln(A_1/A_2) + \ln(A_2/A_3) + \ldots \ln(A_n/A_{n+1})]/n$$

where Δ is the logarithmic damping ratio, A is the amplitude, and n is the number of vibration waves.

The viscosity (η) of the substance had the function of stopping oscillation of the oscillated body, which was in contact with the substance. Curing changed the molecular weight (M). Therefore, as η became greater, the logarithm increased. η was evaluated with the following equations:

$$\eta = kM^{\theta}$$

$$\eta = ke^{\beta/t}$$

where t is the ambient temperature and k, θ, and β are constants.

Figure 3 shows the typical curing curve, as measured with the rigid-body pendulum instrument with theoretical analysis as follows. In curve c, the reaction begins after point 1, and M is increased; therefore, η increases as well. The increasing slope of η between points 3 and 4 shows the velocity of increased η. The first point of inflection is called the gel point, and its corresponding time is the gel time. After point 5, the last point of inflection is called the cure point, and its corresponding time is the cure time, which results in a balanced curve.

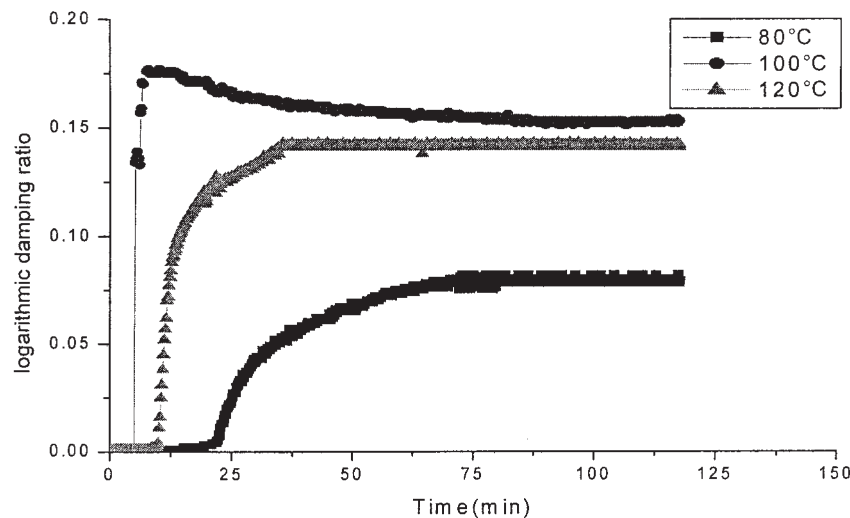

Figure 4 The curing behavior of temperature on (a) 80°C, (b) 100°C, (c) 120°C of silicone.

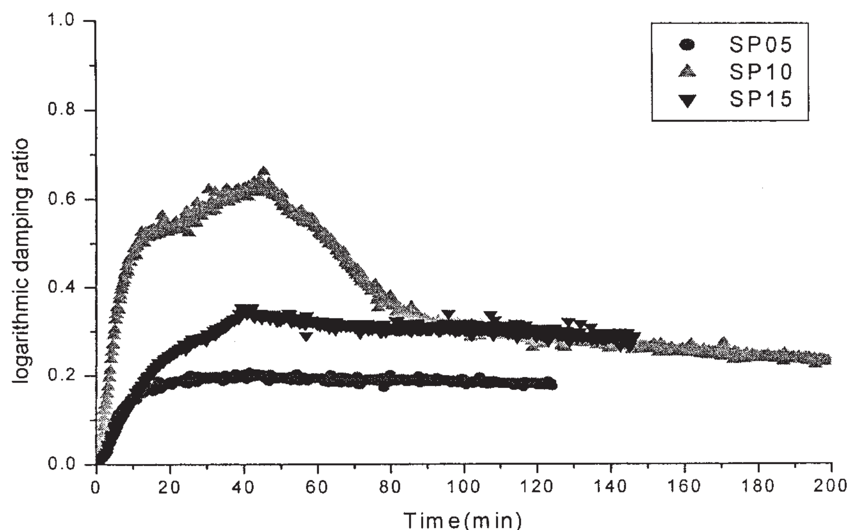

Figure 5 The temperature curing behavior on 150°C of silicone/PEL blends with PEL contents.

Rigid-body pendulum rheometer measurements

The rigid-body pendulum rheometer, Model RPT-alpha 100, manufactured by Tohoku Electronic Industrial Co., Ltd., was used as a measuring instrument. A frame-type pendulum (FRB-100) with a knife-edged (RBE-130) was chosen, and the set up inertia was 500 g cm.

FTIR analysis

Tests were conducted using the FTIR-1 of a Perkin-Elmer™ model. The FTIR was measure under room temperature and the structural changes of the Silicone/PPO-PEO blends were observed.

Differential scanning calorimetery analysis

Thermal analyses were made using a Du Pont DSC910 differential scanning calorimeter (DSC). Under an N_2 flow, the sample was heated to 200°C at 5°C/min, and the heat capacity versus temperature was recorded for each scan.

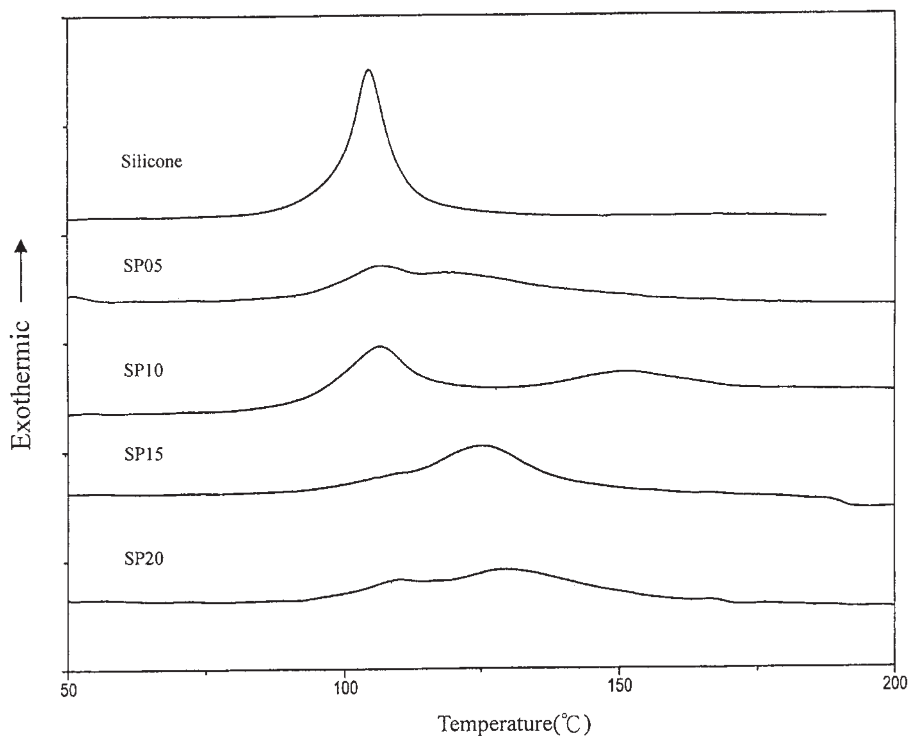

Figure 6 Differential scanning calorimetry curves of silicone/PEL blends with PEL contents.

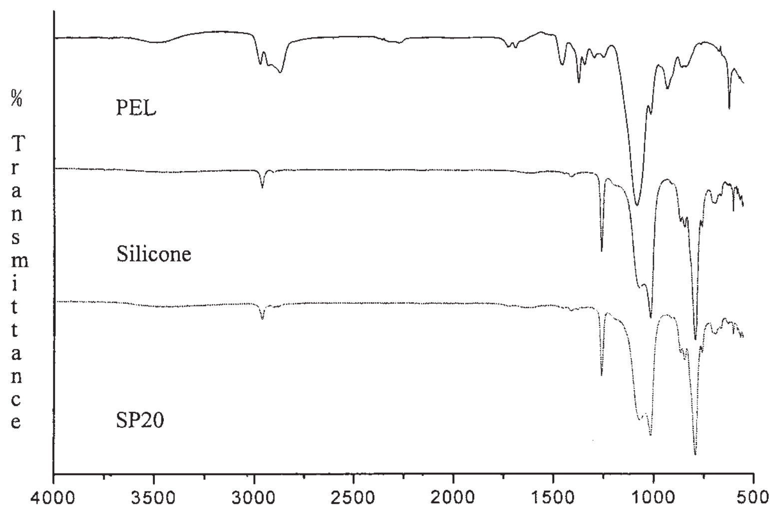

Figure 7 The evaluation by FTIR of silicone/PEL blends with PEL contents.

Mechanical properties of silicone/PEL blends

Tensile stress and strain were measured using a Universal Tensile Tester with a tension velocity of 500 mm/min, ASTMD412C. The hardness was measured with a Durometer Shore A, ASTM D2240.

Dynamic mechanical properties (DMA) analysis

Silicone/PEL/Ppy 3-components polymers were produced 2 mm wide to a specification of $2 \times 10 \times 5$ mm. A DMA model No. TA2980 with a temperature rising rate of 5°C/min from −150 to 150°C under a frequency of 1 Hz was used for temperature scanning. The relationship among the reserved damping (tan δ) and temperature was measured.

Scanning electron microscope (SEM) analysis

The morphology was measured using SEM (England Cambridge S-360). A gold pattern was sputtered onto the sample holder surface and SEM was used to observe the sample.

RESULT AND DISCUSSION

Curing process of silicone/PEL blends

A rigid-body pendulum rheometer was used in the thermal reaction system in this study to observe the changes of the polymer blend curing process from liquid to solid films. Figure 4 shows the curing curves of silicone under different process temperatures. From the curing curve of

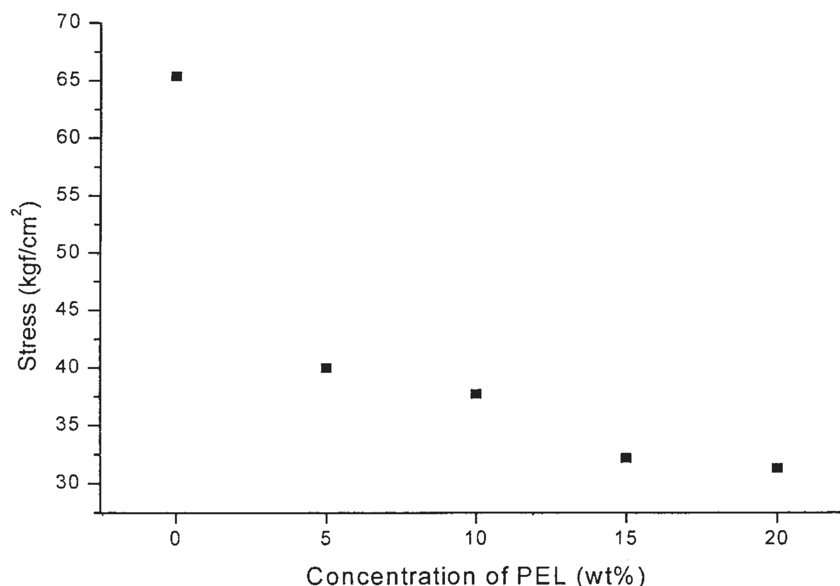

Figure 8 The silicone/PEL blend stress with PEL content.

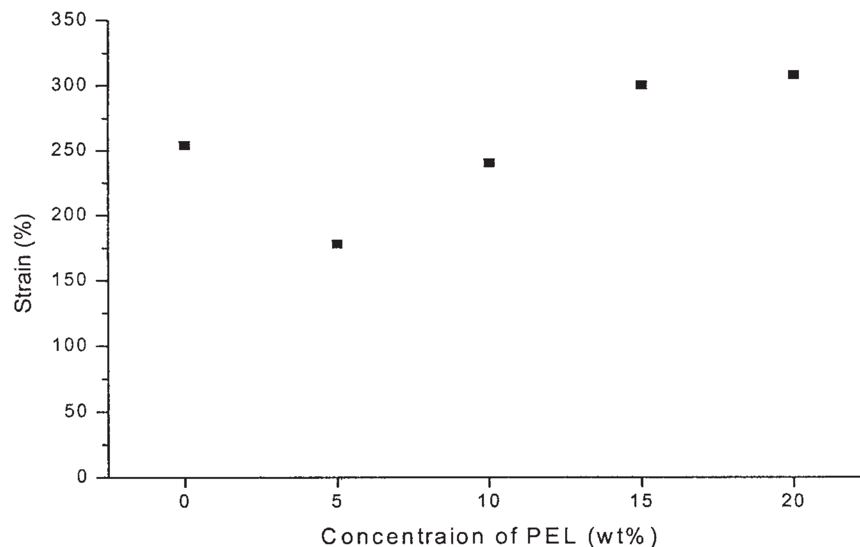

Figure 9 The silicone/PEL blend strain with PEL content.

silicone at 80°C it shows the early stage of the curing process where the logarithmic damping ratio is small; when the reaction time increases, the logarithmic damping ratio starts to rise in about 25 min, and the generation of crosslinking starts. Then there is a transition on the logarithmic damping ratio curve at the initial stage of the reaction, which is called the gel point, and the time corresponding to it is called the gel time. In about 36 min, logarithmic damping ratio curve becomes balanced in the transition process from the liquid to solid films. When the curing temperature rises to 120°C, the silicone network structure is fast to form (about 12 min) and the internal stress is produced. At the end of the curing time, the internal stress disappears slowly, and the logarithmic damping ratio relaxation is balanced. Thus, the curing time is decreased as the curing temperature rises.

On the other hand, silicone with modify PEL contents is shown in Figure 5. It shows PEL obstructs silicone molecular chain crosslinking transformed from liquid to solid films, requiring a higher temperature for curing than silicone. This phenomenon is because the linear PEL polymer chain winds around the silicone network structure. When the curing temperature rises to 150°C, the PEL content increases and the curing time for SP05, SP10, and SP15 becomes 25, 49, and 46 min, respectively. In addition, the SP10 blends curing curve has two transitions. This change indicates the early stage of the curing process at 150°C;

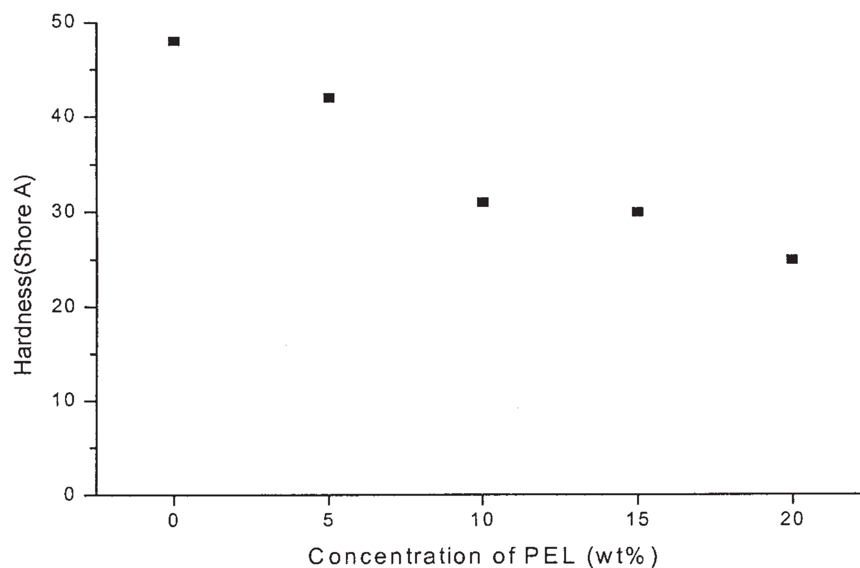

Figure 10 The silicone/PEL blend hardness with PEL content.

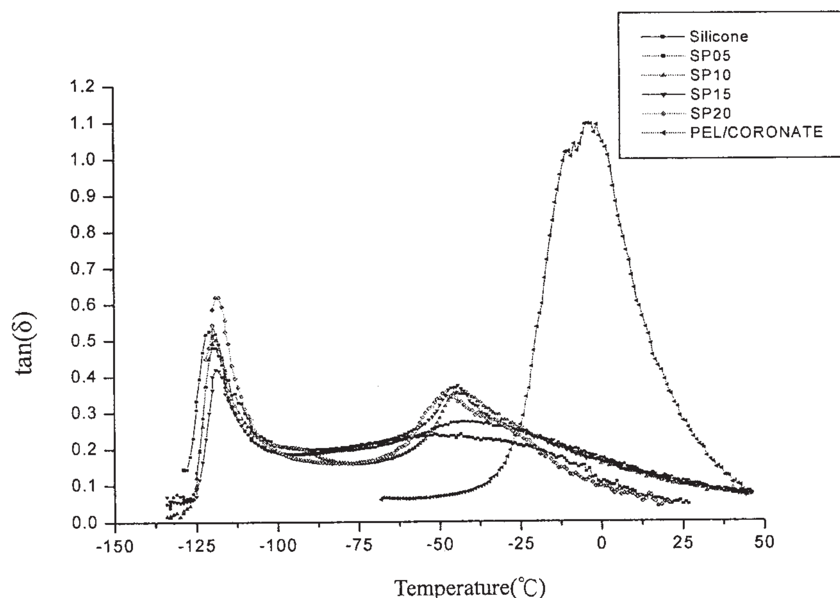

Figure 11 The temperature on tan δ silicone/PEL blend effect with PEL content at 1 Hz.

logarithmic damping ratio is small, in about 2 min, the logarithmic damping ratio starts to rise, which is increasing phenomenon of the logarithmic damping ratio without part of the silicone to process the crosslinking. In about 24 min, this increases the phenomenon of the logarithmic damping ratio without part of PEL wound around the silicone to process the crosslinking. At the last cured time, the internal stress disappears slowly, and the logarithmic damping ratio relaxation is balanced. When the PEL contains 15 wt %, extra lithium cations produce an interaction with the oxygen atom on the silicone polymer chain. The reaction rate is thus slower than SP10 because the polymer chain segments are strongly restricted to lithium cations.

Analysis of the polymer network structure of the silicone/PEL blends

The silicone blends modified with various amounts of PEL are shown in Figure 6. It shows the exothermic peak of silicone at 105°C. When the modifier 5 wt % PEL was blended in the silicone, another exothermic peak appeared at a higher temperature. This is because the linear PEL polymer chains will wind around the silicone polymer network structure. Therefore, the

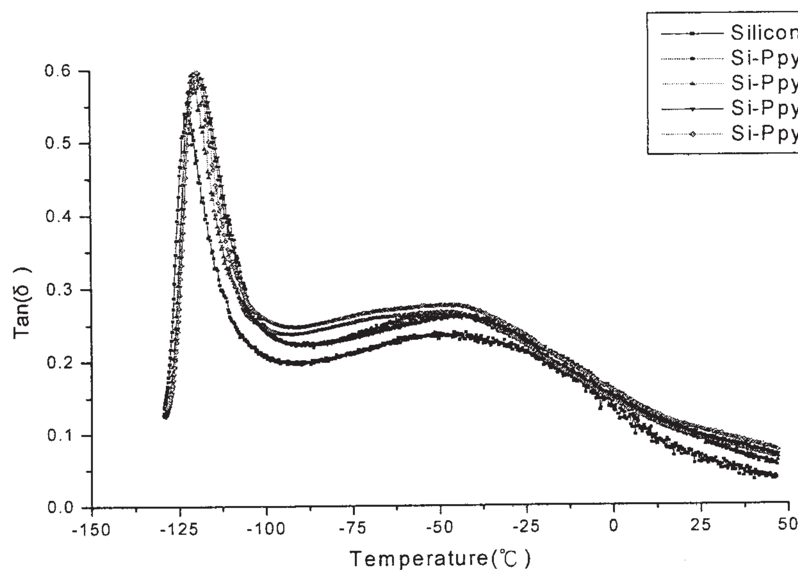

Figure 12 The temperature on tan δ of Ppy on silicone surface effect at 1 Hz (Si—Ppyx, x: dip-coating times of Ppy).

silicone polymer chains need a high temperature to increase the polymer chain's intense movement for forming the crosslinking. When the modifier PEL content is in the range of 10 to 20 wt %, the absorption of lithium cations with oxygen atoms of the silicone polymer chain increases. This may lead to the entire silicone polymer chain crosslinking shift to a higher temperature and the silicone/PEL blends to form a semi-IPN structure.

The silicone/PEL blends with various PEL contents are shown in Figure 7. The figure indicates that the silicone absorption peaks are at 3600 cm^{-1} (Si—OH), 1080 cm^{-1} (Si—O—Si), 2958, 1245, and 802 cm^{-1} (Si—CH_3), and the PEL absorption peak is at 3450 cm^{-1} (—OH). There is no absorption peak formed in the SP20. This reveals that no chemical reaction exists between silicone and PEL. The FTIR results could further explain the formation of silicone/PEL blends to a semi-IPN structure.

Mechanical properties of silicone/PEL blends

Stress and strain curves for silicone with varied PEL contents are shown in Figures 9 and 10. The figure indicates that the stress decreases as the PEL content increases. The in PEL contents, in the range of 5 to 10 wt %, the strain decreases as the linear PEL winds only around the silicone network. This obstructs the silicone polymer chain movement, causing it not to keep up with deformation rate. However, as the PEL content reaches 15 wt %, the strain increases because the plasticating effect produces extra PEL with the silicone. The silicone hardness curve at various PEL contents is shown in Figure 11. This reveals a correlation with the stress bar chart.

TABLE II
The Glass Transition Temperature of Silicone/PEL Blends

Code No./ Temp (°C)	T_{ga}	T_{gb}
Silicone	−123.8	−50.0
SP05	−122.6	−38.9
SP10	−122.0	−40.6
SP15	−121.4	−43.1
SP20	−120.5	−47.3
PEL/coronate	0	—

Intermolecular interaction of silicone/PEL/Ppy composites

Figure 12 is a DMA curve measured at 1 Hz for transformed films of various proportions. The side chains molecular movement temperature (T_{ga}) peak of silicone is at −123.8°C. The main chains molecular movement temperature (T_{gb}) peak is at −50°C. After PEL is crosslinked and cured via cornate, T_{gb} is at 0°C and silicone increases along with the increase in PEL content. Changes in the T_{ga} and T_{gb} peaks are shown in Table II. Upon adding 5wt % of PEL into silicone, the T_{ga} temperature increased from −123.8 to −122.6°C, and the T_{gb} temperature increases from −50.0 to −38.9°C. This is because there is a greater interaction between the linear molecular structure of PEL and the molecular main chain of silicone, which results in T_{gb} temperature increases of about 11°C and crosslinking

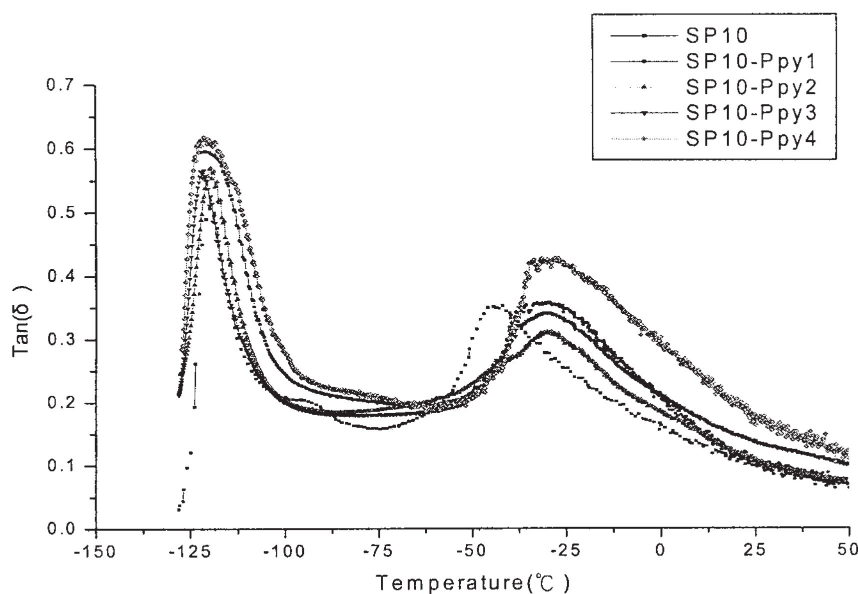

Figure 13 The temperature on tan δ of Ppy on SP10 blend surface at 1 Hz.

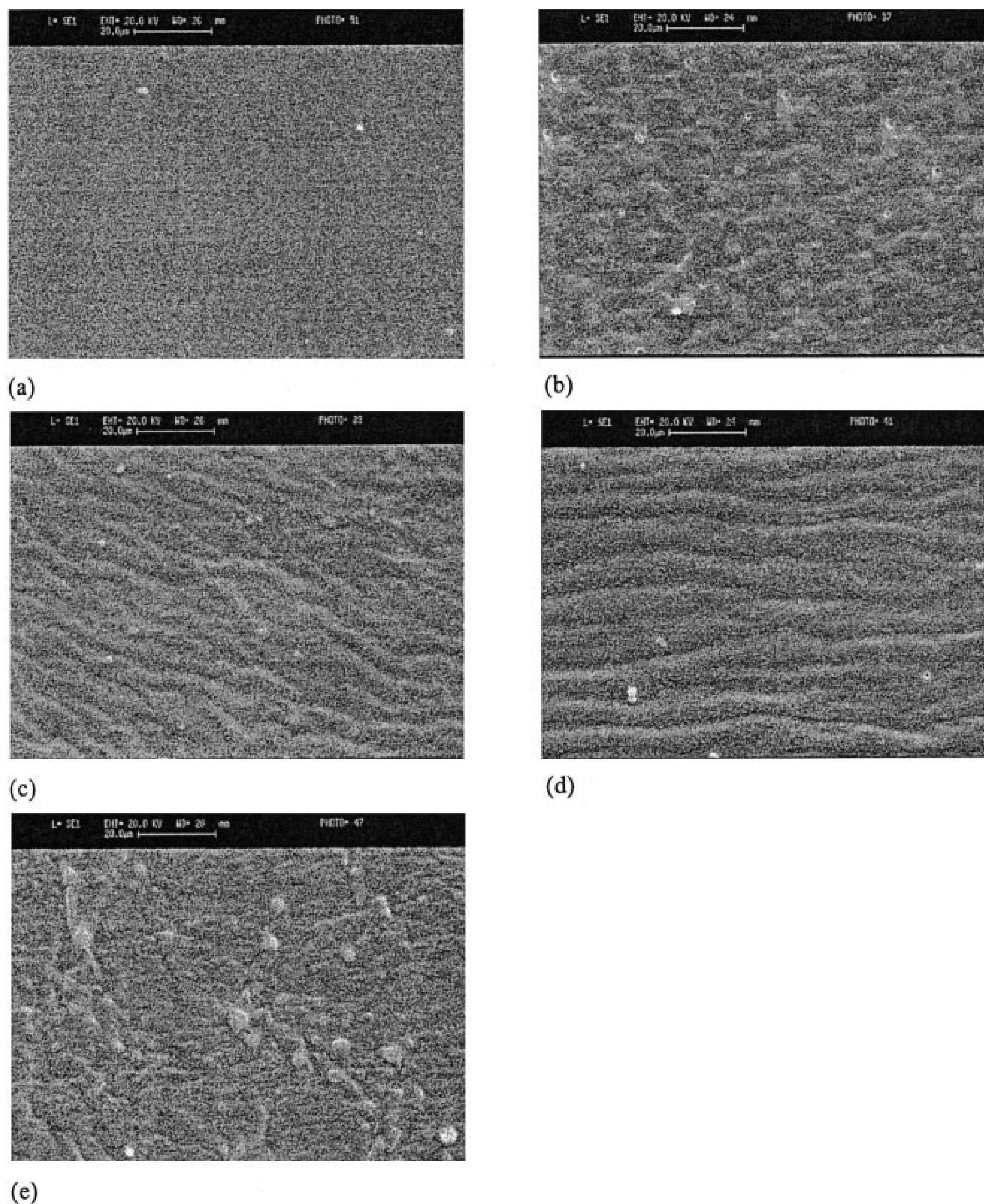

Figure 14 Scanning electron micrographs of silicone/PEL blends with PEL contents (×1000): (a) silicone, (b) SP05, (c) SP10, (d) SP15, (e) SP20.

PEL T_{gb} is at 0°C. Thus, the linear molecular structure of the PEL peak ranges from SP05 and PEL/coronate. As the PEL content reaches 20 wt %, the T_{ga} temperature of silicone increases from −123.8 to −120.5°C, and the PEL peak decreases from −38.9 to −47.3°C. This is because silicone consists of crosslinking polymers, and PEL has linear molecules. When both are blended, the linear PEL polymer chains will winds around the silicone polymer network structure, which results in semi-IPN. Therefore, the temperature of the PEL polymer chain decreased by 9°C and the silicone polymer chain temperature increases by about 3°C as the rigidity of the latter hinders the movement of the silicone polymer chain.

The DMA curve measured at 1 Hz for silicone and SP10 blends for various dip-coating times of Ppy are show as Figures 12–13. As the Ppy membrane become more rigid and has a better interaction with the silicone side chain molecules, the T_{ga} temperature increases by 5°C. However, no significant change occurred for the silicone main chain molecules. There are no significant peak changes as the Ppy dip-coating time increases. Also, the T_{gb} of SP10 increased by 14°C, which indicated the interaction between Ppy and PEL

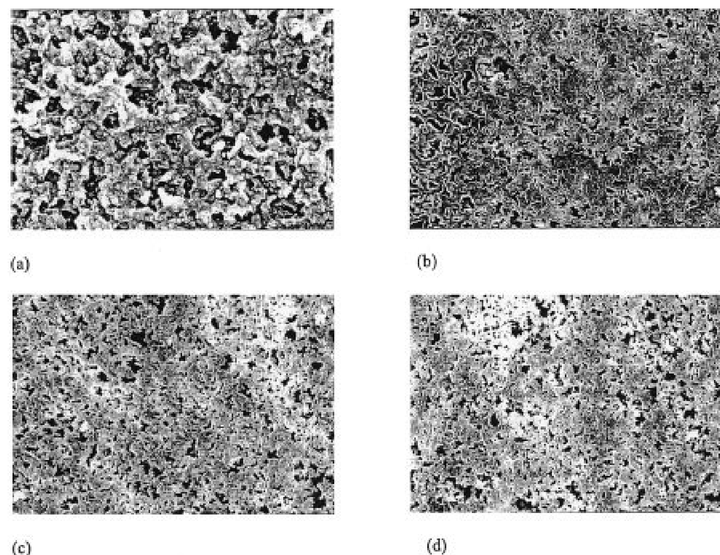

Figure 15 Scanning electron micrographs of Ppy on silicone surfaces (×1000): (a) Si—Ppy1, (b) Si—Ppy2, (c) Si—Ppy3, (d) Si-Ppy4.

is greater than that between Ppy and silicone. There were no significant peak changes as the Ppy dip-coating time increased.

Morphology of silicone/polypyrrole/PEL composites

The SEM surface chart for silicone with various PEL contents are show in Figure 15. The silicone surface is neat, and produced microphase-separated surface structure after adding PEL contents 5 to 20 wt %. Continuous, the SEM surface characterization for the Ppy variety dip-coating number on the silicone and SP10 blends surface are shown in Figures 16 and 17. In numerous past studies,[14–20] coupled with silicone ability, this facilitates their use as a surface modifier to improved silicone surfaces. Our result shows the Ppy membrane becomes even as the surface of the blends surface impregnated in dip-coating number increases. The Ppy film effect on the surface of the SP10 blends is more uniform than that of silicone. This is because of the inherently hydrophobic nature of silicones and the weak intermolecular interaction between the Ppy and silicone polymer. After silicone has been modified, it could produce microphase separation and have inter-

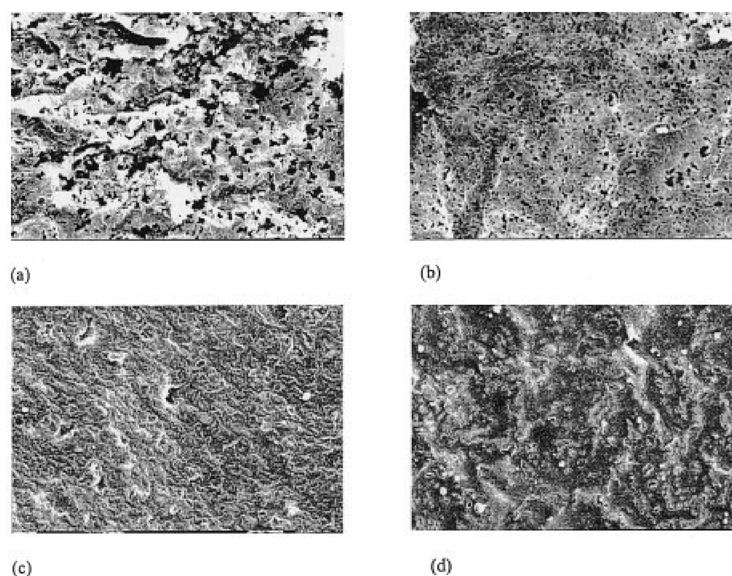

Figure 16 Scanning electron micrographs of Ppy on SP10 blend surfaces (×1000): (a) SP10–PPy1, (b) SP10–Ppy2, (c) SP10–Ppy3, (d) SP10–Ppy4.

molecular interaction between the Ppy and SP10 blends. This leads easily to a Ppy *in situ* polymerization-forming membrane on the SP10 blend surface.

CONCLUSION

The following specific conclusion can be made from the experimental results:

1. According to the changes in various silicone/PEL blends proportions during the curing process, it is known that the curing behavior and the molecular movement properties become different when the blends went from liquid to solid. As PEL reaches 10 wt % content, the curing rate becomes fastest.
2. The FTIR result shows that no chemical reaction exists between silicone and PEL. As the PEL polymer chain winds only around the silicone polymer network structure, the silicone network structure becomes defective, resulting in a decrease in mechanical properties.
3. The DSC analysis indicates that the PEL polymer chain winds around the silicone, which caused increases in the temperature required for silicone polymer chains to crosslink.
4. Two molecular movement temperatures were found in the dynamics analysis of silicone/PEL blends. This reveals that intermolecular interaction exists between the silicone/PEL/Ppy composites, and the intermolecular interaction between Ppy and PEL polymer is greater than that between Ppy and silicone polymer.
5. From the SEM observations, the silicone surface is neat, and produced a microphase-separated surface structure after addition of PEL. In addition, the Ppy membrane effect on the surface of SP10 blends is more even and delicate that that on the silicone surface.

References

1. Ohiberg, S. M.; Alexander, L. E.; Warrick, E. L. J Polym Sci 1958, 27, 1.
2. Polmantee, K. E.; Hunter, M. J. J Appl Polym Sci 1959, 1, 3.
3. Hagerman, E. M. J Appl Polym Sci 1969, 13, 1873.
4. Matsuo, M.; Kondo, Y. Polym Eng Sci, 1970, 10, 253.
5. Polmanteer, K. E. Rubber Chem Tech 1981, 54, 1051.
6. Yin, W. S.; Liu, H. W.; Gan, L. H. J Appl Polym Sci 1999, 72, 1 95.
7. Eaborn, C. Organosilicon Compound; Butteworths: London, 1962; p 100.
8. Noll, W. Chemistry and Technology of Siloxanes; Academic: New York, 1968; p 17.
9. Chiang, C. K. Polym Commun 1981, 22, 1454.
10. Hooper, A.; North, J. M. Solid State Ionics 1983, 9–10, 1161.
11. Gauthier, M.; Fauteux, D.; Vassort, G.; Belanger, A.; Duval, M.; Ricoux, P.; Chabagno, J. M.; Muller, D. Rigaud, P. Armand, M. B.; Deroo, D. J Appl Polym Sci 1985, 132, 1333.
12. Skotheim, T. A; Inganas, O. J Electrochem Soc 1985, 132, 2116.
13. Abraham, K. M.; Alamgir, M.; Perrotti, S. J. J Electrochem Soc 1988, 135, 535.
14. West, K.; Zachau-Christiansen, B.; Jacobsen, T.; Atlung, S. J Electrochem Soc 1985, 132, 3061.
15. Medalia, A. I Rubber Chem Technol 1986, 59, 432.
16. Polley, M. H.; Boonstra, B. B. Rubber Chem Technol 1957, 30, 170.
17. Rani Joseph, K. G.; Sudha Kartha, C. J Appl Polym Sci 1998, 69, 1043.
18. Kost, J.; Narkis, M.; Foux, A. Polym Eng Sci 1983, 23, 10, 567.
19. Kost, J.; Narkis, M.; Foux, A. J Appl Polym Sci 1984, 29, 3937.
20. Kost, J.; Narkis, M.; Foux, A. Polym Eng Sci 1994, 34, 21, 1628.
21. Kim, N. Y.; Laibinis, P. E. J Am Chem Soc 1999, 121, 7162.
22. Gan, L. H.; Gan, Y. Y.; Yin, W. S. Polymer 1999, 40, 4035.
23. Tanaka, T. Coating Films Evaluation of Physical Property; Ricogaka: Japan, 1993.
24. Tanaka, T. Proceedings of the International Pressure Sensitive Adhesive Technoforum; Tokyo, Japan, 1997; p 143.
25. Clark, D. T.; Peeling, J.; O'Mallery, J. M. J Polym Sci Part: A Polym Chem Ed 1976, 14, 543.
26. Bott, R. H.; Summers, J. D.; Arnold, C. A.; Talor, L. T.; Ward, T. C.; McGrath, J. E. J Adhesion 1987, 23, 67.
27. Yilgor, I.; Steckle, W. P.; Yilgor, E., Jr.; Freelin, R. G; Riffle, J. S. J Polym Sci Part: A Polym Chem Ed 1989, 27, 3673.
28. Ezuka, Y.; Ono, T.; Imai, K J Colloid Interface Sci 1990, 136, 408.
29. Kobayashi, H. J Colloid Interface Sci 1993, 156, 294.
30. Schmitt, R. L.; Gardella, J. A., Jr.; Magill, J. H.; Salvati, L., Jr.; Chin, R. L. Macromolecules 1985, 18, 2675.
31. Tsai, M. F.; Lee, Y. D.; Ling, Y. C. J Appl Polym Sci 1998, 10, 1669.